Research Article

MOLECULAR PAIN

Molecular Pain
Volume 12: 1–16

DOI: 10.1177/1744806916682242
journals.sagepub.com/home/mpx
SAGE

G9a inhibits CREB-triggered expression of mu opioid receptor in primary sensory neurons following peripheral nerve injury

Lingli Liang, MD, PhD[1], Jian-Yuan Zhao, PhD[1,2], Xiyao Gu, PhD[1], Shaogen Wu, MD, PhD[1], Kai Mo, MD, PhD[1], Ming Xiong, MD, PhD[1], Brianna Marie Lutz, BS[1], Alex Bekker, MD, PhD[1] and Yuan-Xiang Tao, MD, PhD[1,3,4]

Abstract

Neuropathic pain, a distressing and debilitating disorder, is still poorly managed in clinic. Opioids, like morphine, remain the mainstay of prescribed medications in the treatment of this disorder, but their analgesic effects are highly unsatisfactory in part due to nerve injury-induced reduction of opioid receptors in the first-order sensory neurons of dorsal root ganglia. G9a is a repressor of gene expression. We found that nerve injury-induced increases in G9a and its catalyzed repressive marker H3K9m2 are responsible for epigenetic silencing of *Oprm1*, *Oprk1*, and *Oprd1* genes in the injured dorsal root ganglia. Blocking these increases rescued dorsal root ganglia *Oprm1*, *Oprk1*, and *Oprd1* gene expression and morphine or loperamide analgesia and prevented the development of morphine or loperamide-induced analgesic tolerance under neuropathic pain conditions. Conversely, mimicking these increases reduced the expression of three opioid receptors and promoted the mu opioid receptor-gated release of primary afferent neurotransmitters. Mechanistically, nerve injury-induced increases in the binding activity of G9a and H3K9me2 to the *Oprm1* gene were associated with the reduced binding of cyclic AMP response element binding protein to the *Oprm1* gene. These findings suggest that G9a participates in the nerve injury-induced reduction of the *Oprm1* gene likely through G9a-triggered blockage in the access of cyclic AMP response element binding protein to this gene.

Keywords

G9a, opioid receptor, dorsal root ganglion, nerve injury

Date received: 10 August 2016; revised: 20 October 2016; accepted: 31 October 2016

Introduction

Neuropathic pain is a distressing and debilitating disorder.[1] It is characterized by spontaneous ongoing or intermittent burning pain, an enhanced response to noxious stimuli (hyperalgesia), and pain in response to normally innocuous stimuli (allodynia). Currently, this disorder is still poorly managed. Opioids, like morphine, remain the mainstay of prescribed medications in the treatment of neuropathic pain. However, a majority of neuropathic pain patients show unsatisfactory pain relief.[2] They often require repeated and prolonged administration of higher doses of opioids. However, such opioid regimens lead to nausea, constipation, respiratory depression, opioid analgesic tolerance and hyperalgesia, respiration inhibition, and additional

[1]Department of Anesthesiology, New Jersey Medical School, Rutgers, The State University of New Jersey, Newark, NJ, USA
[2]State Key Laboratory of Genetic Engineering, Collaborative Innovation Center for Genetics and Development, School of Life Sciences, Fudan University, Shanghai, China
[3]Department of Cell Biology & Molecular Medicine, New Jersey Medical School, Rutgers, The State University of New Jersey, Newark, NJ, USA
[4]Department of Physiology, Pharmacology & Neuroscience, New Jersey Medical School, Rutgers, The State University of New Jersey, Newark, NJ, USA

Corresponding author:
Yuan-Xiang Tao, Department of Anesthesiology, New Jersey Medical School, Rutgers, The State University of New Jersey, 185 S. Orange Avenue, MSB, E-661, Newark NJ 07103, USA.
Email: yuanxiang.tao@njms.rutgers.edu

side-effects.[3] These adverse side effects significantly limit opioid use in neuropathic pain patients. Studies on neurobiological mechanisms of neuropathic pain suggest that nerve injury-induced reduction of opioid receptor mRNA and protein expression in the injured dorsal root ganglion (DRG) may be responsible, at least in part, for the decreased analgesic effects of opioids in neuropathic pain patients.[4–7] Therefore, an understanding of how nerve injury drives DRG opioid receptor reduction may improve opioid analgesic efficacy and propose novel therapeutic strategies for managing neuropathic pain.

Epigenetic modifications including histone methylation control gene expression.[8] The histone methyltransferase G9a causes dimethylation on histone H3 on lysine residue 9 (H3K9me2), resulting in condensed chromatin and gene transcriptional repression.[9,10] G9a has recently been associated with nerve injury-induced epigenetic silencing of mu opioid receptor (MOR) in DRG.[11] However, whether G9a also participates in the nerve injury-induced downregulation of other opioid receptors in the DRG is unclear. Furthermore, how G9a participates in nerve injury-induced DRG MOR reduction is still unknown.

Here, we first confirmed whether nerve injury-induced increases in G9a and its catalyzed repressive marker, H3K9me2, were responsible for nerve injury-induced reductions of MOR as well as kappa opioid receptor (KOR) and delta opioid receptor (DOR) in the injured DRG. We then examined whether these increases were associated with the enhancement of MOR-gated primary afferent neurotransmitter release and the decrease of MOR-mediated analgesia following peripheral nerve injury. Finally, we elucidated the mechanism of how G9a leads to DRG MOR downregulation under neuropathic pain conditions.

Materials and methods

Animal preparations

C57BL/6 J wild-type mice, Avil$^{Cre/+}$ mice, and G9a$^{fl/fl}$ mice and Sprague Dawley (SD) rats were used in this study. G9a$^{fl/fl}$ mice (provided by Dr. Eric J Nestler, Icahn School of Medicine at Mount Sinai, New York, USA) were fully backcrossed to C57BL/6 J mice and were homozygous for a floxed G9a allele. Male Avil$^{Cre/+}$ mice (provided by Dr. Fan Wang, Duke University Medical Center, Durham, NC) were crossed with G9a$^{fl/fl}$ mice to obtain G9a conditional knockout (G9aKO) mice. All animals were kept in a standard 12-h light/dark cycle, with water and food pellets available *ad libitum*. Male mice weighing 25–30 g and male rats weighing 250–300 g were used for behavior testing. All procedures used were approved by the Animal Care and Use Committee at Rutgers New Jersey Medical School and are consistent with the ethical guidelines of the US National Institutes of Health and the International Association for the Study of Pain. All efforts were made to minimize animal suffering and to reduce the number of animals used. All of the experimenters were blind to treatment condition.

DRG microinjection

DRG microinjection was carried out as described[12,13] with minor modification. Briefly, a midline incision was made in the lower lumbar back region, and the L_3 and/or L_4 articular processes were exposed and then removed with small ronguers. After the DRG was exposed, viral solution (0.5–1 μl) was injected into one site in the L_3 and/or L_4 DRGs with a glass micropipette connected to a Hamilton syringe. The pipette was removed 10 min after injection. The surgical field was irrigated with sterile saline and the skin incision closed with wound clips. The injected mice displayed no sign of paresis or other abnormalities. The immune responses from viral injection were thus minimal.

Neuropathic pain models

A mouse neuropathic pain model of unilateral L_4 spinal nerve ligation (SNL) was carried out as described previously.[14] Briefly, a midline skin incision was made on the lower back. The fifth lumbar transverse process was identified and then was separated from its muscle attachments. The underlying fourth lumbar spinal nerve was isolated and ligated with a 7-0 silk suture. The ligated nerve was then transected at the distal end. Sham-operated groups received identical surgical procedures only exposing the nerves without ligation and transection. The surgical field was then irrigated with sterile saline, and the skin incision was closed with wound clips.

Intrathecal catheter implantation in rats and drug administration

A polyethylene 10 catheter was inserted into the subarachnoid space as described.[15] After seven days of recovery, L5 SNL or sham surgery was carried out. Saline or BIX01294 (Cayman Chemical, Ann Arbor, Michigan) was intrathecally injected before surgery and once daily after surgery for seven days.

Models of morphine-induced tolerance and abnormal pain hypersensitivity

Morphine tolerance was induced in mice as described.[16] Briefly, mice received subcutaneous (s.c.) injection of morphine (20 mg/kg; WEST-WARD, Eatontown, NJ)

twice daily (at a 12-h interval) for nine consecutive days in naïve mice or twice daily for four consecutive days starting on day 6 post-SNL. The tail flick test as described below was performed before morphine injection and at 0.5 h after s.c. injection of an inducing dose of morphine (10 mg/kg in naïve mice and 3 mg/kg in SNL mice) on mornings 1, 3, 5, and 9 in naïve mice or on mornings 6, 8, and 10 after SNL. The morphine-treated time for the tail flick test was 1 h earlier than the morphine-treated time for the tolerance development in the morning. Cumulative dose-response curves were performed as described previously[16] on the afternoon of the last day. Mice received a very low morphine dose (1 mg/kg, s.c.) and the analgesic effect was assessed 30 min later by the tail flick test. Mice that were not analgesic at the first dose then received a second dose (cumulative dosing increase of 0.3 log units) and were tested 30 min afterward. The analgesic effect was observed until the mice did not show a tail flick response at the cut-off time or no further increase in tail-flick latency occurred from one dose to the next dose. Morphine-induced mechanical and thermal pain hypersensitivities in naïve mice were observed as described;[16] 20 mg/kg morphine were subcutaneously injected twice daily for eight days. Mechanical and thermal behavioral tests as described below were carried out prior to morphine injection and on days 1, 2, and 4 after morphine withdrawal.

Loperamide-induced tolerance and abnormal pain hypersensitivity

The protocol of loperamide tolerance in mice was modified based on the protocol in rats.[17] Loperamide hydrochloride (Sigma–Aldrich, St. Louis, MO) was dissolved in 6.7% 2-hydroxypropyl-β-cyclodextrin (CDEX, 20% in w/v in sterile water) and 6% dimethyl sulfoxide (DMSO). Mice received subcutaneous (s.c.) injection of loperamide (10 mg/kg) twice daily for five consecutive days in naïve mice or twice daily for three consecutive days starting on day 6 post-SNL (at a 12-h interval). The paw withdrawal latency as described below was performed before loperamide injection and at 0.5 h after s.c. injection on mornings 1, 3, and 5 in naïve mice or on mornings 7, 8, and 9 after SNL.

Behavioral tests

The tail flick test was carried out to observe the morphine tolerance development. A tail-flick apparatus (Model 33B Tail Flick Analgesy Meter, IITC Life Science, Woodland Hills, CA, USA) with a radiant heat source connected to an automatic timer was used to assess the analgesic response.[16] A cut-off time latency of 10 s was used to avoid tissue damage to the tail. Tail-flick latencies were measured as the time required to induce a tail flick after applying radiant heat to the skin of the tail. The antinociceptive effects were expressed as the percentage of maximal possible analgesic effect (% MPAE): % MPAE = [(response latency − baseline latency) / (cut-off latency − baseline latency)] × 100%.

Mechanical behavioral test was carried out as described.[12,13,16,18] Briefly, each mouse was placed in a Plexiglas chamber on an elevated mesh screen. One calibrated von Frey filament (1.47 mN; Stoelting Co., Wood Dale, IL, USA) was applied to the hind paw for approximately 1 s, and each stimulation was repeated 10 times to both hind paws. The occurrence of paw withdrawal in each of these 10 trials was expressed as a percent response frequency [(number of paw withdrawals/10 trials) × 100 = % response frequency], and this percentage was used as an indication of the amount of paw withdrawal.

Thermal behavioral test was carried out as described.[12,13,16,18] In brief, each mouse was placed in a Plexiglas chamber on a glass plate. A radiant heat from Model 336 Analgesic Meter (IITC Inc./Life Science Instruments, Woodland Hills, CA, USA) was applied by aiming a beam of light through a hole in the light box through the glass plate to the middle of the plantar surface of each hind paw. When the animal lifted its foot, the light beam was turned off. The length of time between the start of the light beam and the foot lift was defined as the paw withdrawal latency. Each trial was repeated five times at 5-min intervals for each side. A cut-off time of 20 s was used to avoid tissue damage to the hind paw.

Plasmid constructs and virus production

Mouse full-length CREB (cyclic AMP response element binding protein) cDNA was synthesized and amplified from total RNA of mouse DRG using the SuperScript III One-Step RT-qPCR System with the Platinum Taq High Fidelity Kit (Invitrogen/ThermoFisher Scientific, Grand Island, NY) and primers (Table 1). Fragments harboring CREB were ligated into pro-viral plasmids using the BspEI and NotI restriction sites. The resulting vector expressed CREB under the control of the cytomegalovirus promoter. AAV5 viral particles carrying full-length CREB cDNA were produced at the UNC Vector Core. AAV5-GFP and AAV5-Cre were purchased from UNC Vector Core (Chapel Hill, NC). HSV-GFP and HSV-G9a were provided by Dr. Eric J Nestler.

DRG neuronal culture and transfection

Primary DRG neuronal cultures and viral transfection were carried out as described.[13] Briefly, adult mice were euthanized with isoflurane and all DRG were collected in

Table 1. All primers used.

Names	Sequences	Names	Sequences
Real-time RT-PCR and single cell RT-PCR		ChIP-PCR	
Ehmt2-F	5'-AAATTGGGAACTTGGAAATGG-3'	*Ehmt2*promoter-F	5'-GCACCCGAGGGCAGCAGT-3'
Ehmt2-R	5'-CACTACCCGTGAAGGAGGC-3'	*Ehmt2*promoter-R	5'-CCAGCAAGGCGTCACTCCC-3'
Oprm1-F	5'-TCTTCACCCTCTGCACCATG-3'	*Oprm1F1-F*	5'-GGCACATGAAACAGGCTTCT-3'
Oprm1-R	5'-TCTATGGACCCCTGCCTGTA-3'	*Oprm1F1-R* 5'-ACCCACA TCCCCATATCTGA-3'	
Oprd1-F	5'-TTTGGCATCGTCCGGTACAC-3'	*Oprm1F2-F*	5'-CCTCAGATATGGGGATGTGG-3'
Oprd1-R	5'-AGAGCACAGCCTTGCACAGC-3'	*Oprm1F2-R*	5'-ATCAGCCAGGAAAGTCGTTG-3'
Oprk1-F	5'-AGTGTGGACCGCTACATTGCT-3'	*Oprm1F3-F*	5'-TGAGTCGGAAGAGTGTTGAGG-3'
Oprk1-R	5'-CAATGACATCCACATCTTCCCTG-3'	*Oprm1F3-R* 5'-CAGAGAGGG TGGGAAGAGAG-3'	
Gapdh-F	5'-TCGGTGTGAACGGATTTGGC-3'	*Oprm1F4-F*	5'-GGAGGCTGATTCTGAGTTGC-3'
Gapdh-R	5'-TCCCATTCTCGGCCTTGACT-3'	*Oprm1F4-R*	5'-TGAGCGTCCGATATTCTCCT-3'
Cloning		*Oprm1F5-F*	5'-TGGTTCCACTAGGGCTTGTC-3'
Creb-RT-F	5'-GGAGCTTGTACCACCGGTAA-3'	*Oprm1F5-R*	5'-CTAAGGGGTCAGAGCAGTCG-3'
Creb-RT-R	5'-CTTGAGGGCAGAAGTGGAAG-3'		
Creb-N-PCR-F	5'-ATATCCGGAGCCACCATGACCA TGGAATCTGGA-3 '		
Creb-N-PCR-R	5'-CGCCAGCGGCCGCAATTAATC TGATTTGTGG-3'		

RT: Reverse-transcription. F: Forward. F1-5: Fractions 1-5. R: Reverse. N-PCR: Nested PCR. Underlined letters: the restriction enzyme recognition sites.

cold Neurobasal Medium (Gibco/ThermoFisher Scientific) with 10% fetal bovine serum (JR Scientific, Woodland, CA), 100 units/ml Penicillin, 100 µg/ml Streptomycin (Quality Biological, Gaithersburg, MD) and then treated with enzyme solution (5 mg/ml dispase, 1 mg/ml collagenase type I in Hanks' balanced salt solution (HBSS) without Ca^{2+} and Mg^{2+} (Gibco/ ThermoFisher Scientific)). After trituration and centrifugation, dissociated cells were resuspended in mixed Neurobasal Medium and plated in a six-well plate coated with 50 µg/ml poly-D-lysine (Sigma, St. Louis, MO). The cells were incubated at 95% O_2, 5% CO_2, and 37°C. One day later, 0.5µl of virus (titer $\geqslant 1 \times 10^{12}$/ ml) was added to each 2-ml well. Neurons were collected two to three days later.

Reverse transcription (RT)-PCR

For quantitative real-time RT-PCR, four unilateral mouse DRG were pooled together to achieve enough RNA. Total RNA was extracted by the Trizol method (Invitrogen/ThermoFisher Scientific), treated with DNase I (New England Biolabs, Ipswich, MA), and reverse-transcribed using the ThermoScript reverse transcriptase (Invitrogen/ThermoFisher Scientific), random hexamers, and oligo (dT) primers or specific RT-primers (Table 1). Template (1 µl) was amplified by real-time PCR using the primers listed in Table 1 (Integrated DNA Technologies). *Gapdh* mRNA was used as an internal control for normalization. Each sample was run in triplicate in a 20 µl reaction with 250 nM forward and reverse primers, 10 µl of SsoAdvanced Universal SYBR Green Supermix (Bio-Rad Laboratories, Hercules, CA) and 20 ng of cDNA. Reactions were performed in a BIO-RAD CFX96 real-time PCR system. Ratios of ipsilateral-side mRNA levels to contralateral-side mRNA levels were calculated using the ΔCt method ($2^{-\Delta\Delta Ct}$). All data were normalized to *gapdh* mRNA, which has been demonstrated to be stable even after peripheral nerve injury insult.[12,13]

For single-cell RT-PCR, freshly dissociated mouse DRG neurons were first prepared as described previously.[13,18] Briefly 4 h after plating, a single living small DRG neuron was collected under an inverted microscope fit with a micromanipulator and microinjector and placed in a PCR tube with 5–10 µl of cell lysis buffer (Signosis, Sunnyvale, CA). After centrifugation, the supernatants were collected. The remaining real-time RT-PCR procedure was carried out according to the manufacturer's instructions with the single-cell real-time RT-PCR assay kit (Signosis). All primers used are listed in Table 1.

Chromatin immunoprecipitation (ChIP) assay

The ChIP assays were conducted using the EZ ChIP Kit (Upstate/EMD Millipore, Darmstadt, Germany) as

described.[13] The homogenization solution from DRG was crosslinked with 1% formaldehyde for 10 min at room temperature. The reaction was terminated by the addition of 0.25 M glycine. After centrifugation, the collected pellet was lysed by SDS lysis buffer with protease inhibitor cocktail and sonicated until the DNA was broken into fragments with a mean length of 200 to 1000 bp. The fragment sizes were verified by gel electrophoresis (data not shown). After the samples were precleaned with protein G agarose, they were subjected to immunoprecipitation overnight with 2 μg of rabbit antibodies against G9a (Abcam, Cambridge, MA), CREB (Abcam), and H3K9me2 (Abcam), or with 2 μg of normal rabbit serum overnight at 4°C. Input (10%–20% of the sample for immunoprecipitation) was used as a positive control. The DNA fragments were purified and identified using PCR/Real-time PCR with the primers listed in Table 1.

Single- or double-labeled immunohistochemistry

Mice were anesthetized with isoflurane and perfused with 4% paraformaldehyde before being analyzed by single- or double-labeled immunohistochemistry. L3 and L4 DRG were removed, post-fixed, and dehydrated before frozen sectioning at 20 μm. After the sections were blocked for 1 h at room temperature in 0.01 M PBS containing 10% goat serum and 0.3% Triton X-100, they were incubated with the following one or two primary antibodies over one or two nights at 4°C. The antibodies include rabbit anti-G9a (1:20, Abcam), mouse anti-CREB (1:100, Cell Signaling, Danvers, MA), guinea pig anti-MOR (1:1,000, EMD Millipore, German), and rabbit anti-KOR (1:200, Novus Biologicals, Littleton, CO). The sections were then incubated with either goat anti-rabbit antibody conjugated to Cy3 (1:200, Jackson ImmunoResearch, West Grove, PA), or goat anti-mouse antibody conjugated to Cy2 (1:200, Jackson ImmunoResearch) or goat anti-guinea pig antibody conjugated to Cy3 (1:200, Jackson ImmunoResearch) for 2 h at room temperature. Control experiments included substitution of normal mouse or rabbit serum for the primary antiserum and omission of the primary antiserum. All immunofluorescence-labeled images were examined using a Leica DMI4000 fluorescence microscope and captured with a DFC365FX camera (Leica, Germany). Single- or double-labeled neurons were quantified manually or by using NIH Image J Software.

Western blotting

Two unilateral mouse DRGs were pooled to reach a suitable total protein concentration. Tissues were homogenized and the cultured cells ultrasonicated in chilled lysis buffer (10 mM Tris, 1 mM phenylmethylsulfonyl fluoride, 5 mM $MgCl_2$, 5 mM EGTA, 1 mM EDTA, 1 mM DTT, 40 μM leupeptin, 250 mM sucrose). After centrifugation at 4°C for 15 min at 1,000 g, the supernatant was collected for cytosolic proteins and the pellet for nuclear proteins. The contents of the proteins in the samples were measured using the Bio-Rad protein assay (Bio-Rad) and then the samples were heated at 99°C for 5 min and loaded onto a 4%–15% stacking/7.5% separating SDS-polyacrylamide gel (Bio-Rad). The proteins were then electrophoretically transferred onto a polyvinylidene difluoride membrane (Bio-Rad). After the membranes were blocked with 3% nonfat milk in Tris-buffered saline containing 0.1% Tween-20 for 1 h, the following primary antibodies were used: rabbit anti-MOR (1:500, Neuromics, Minneapolis, MN), rabbit anti-KOR (1:500, Santa Cruz, Dallas, Texas), rabbit anti-GAPDH (1:1,000, Santa Cruz), rabbit anti-CREB (1:1,000, Abcam), mouse anti-phospho-CREB (Ser133) (1:1,000, EMD Millipore), mouse anti-α-tublin (1:1,000, Santa Cruz), rabbit anti-G9a (1:1,000, Cell signaling), rabbit anti-H3K9me2 (1:500, EMD Millipore), and rabbit anti-histone H3 (1:1,000, Cell Signaling), The proteins were detected by horseradish peroxidase–conjugated anti-mouse or anti-rabbit secondary antibody (1:3,000, Jackson ImmunoResearch) and visualized by western peroxide reagent and luminol/enhancer reagent (Clarity Western ECL Substrate, Bio-Rad) and exposure by ChemiDoc XRS System with Image Lab software (Bio-Rad). The intensity of blots was quantified with densitometry using Image Lab software (Bio-Rad). All cytosol protein bands were normalized to either β-actin, α-tubulin, or GAPDH, whereas all nucleus protein was normalized to total histone H3.

Whole-cell patch clamp recording on spinal cord slices

Adult mouse spinal cord slices were prepared as described.[19] Briefly, mice (age >24 days) were deeply anesthetized with isoflurane. Laminectomy was applied from mid thoracic to lower lumbar levels. The spinal cord was quickly removed and placed in cold modified artificial cerebrospinal fluid (ACSF) containing: (in mM) 80 NaCl, 2.5 KCl, 1.25 NaH_2PO_4, 0.5 $CaCl_2$, 3.5 $MgCl_2$, 25 $NaHCO_3$, 75 sucrose, 1.3 Ascorbate, 3.0 Sodium Pyruvate, oxygenated with 95% O_2 and 5% CO_2 (pH 7.4, 310–320 mOsm). Transverse 350 μm slices for miniature EPSC (mEPSC) recording or 500 μm slices with attached L3/4 dorsal root for evoked EPSC (eEPSC) recording were cut by a vibratome VT-1200 (Leica). Slices were incubated at least 1 h at room temperature in the recording solution containing: (in mM) 125 NaCl, 2.5 KCl, 2 $CaCl_2$, 1 $MgCl_2$, 1.25 NaH_2PO_4, 26 $NaHCO_3$, 25 D-glucose, 1.3 Ascorbate, 3.0 Sodium Pyruvate, oxygenated with 95% O_2 and 5% CO_2 (pH 7.4, 310–320 mOsm).

Whole-cell patch recording was carried out as described.[19] The slice was transferred to a recording chamber (Warner Instruments, Hamden, CT) and perfused with oxygenated recording solution at a rate of 3 ml/min at room temperature. Neurons were identified by infrared differential interference contrast (IR-DIC) with an upright microscope DM6000 (Leica) equipped with a 40×0.80 NA water-immersion objective and a CCD camera (Leica). Whole-cell patch clamp recording was carried out in the voltage-clamp mode. The electrode resistances of micropipettes ranged from 3 to 8 MΩ. Lamina II neurons were clamped with an Axopatch-700B amplifier (Molecular Devices, Downingtown, PA). The intracellular pipette solution contained: (in mM) 110 Cs_2SO_4, 5 TEA-Cl, 0.5 $CaCl_2$, 2 $MgCl_2$, 5 EGTA, 5 HEPES, 5 TEA, 5 MgATP, 0.5 NaGTP, and 1 GDP-β-S. Cs, and TEA was used as a K^+-channel blocker and GDP-β-S used as a GTP binding protein blocker to prevent the postsynaptic μ-opioid mediated effect as previously described.[20–22] To record mEPSC, 500 nM TTX was presented at the recording solution as described above. To record eEPSC, a suction electrode (A-M systems) was used for electrical stimulation of the attached dorsal root. Stimulation was delivered by the suction electrode with a constant current stimulator S88 (Grass, Rockland, MA). To verify different primary afferent inputs, Aβ fiber-evoked EPSCs were classified as monosynaptic by constant latency and absence of failures upon 25 μA/20 Hz stimulation; Aδ fiber-evoked EPSCs were classified as monosynaptic by constant latency and absence of failures upon 100 μA/2 Hz stimulation; C fiber-evoked EPSCs were classified as monosynaptic by absence of failures upon 500 μA/1 Hz stimulation. The conduction velocity was further measured to distinguish the primary afferent input (C < 0.8 m/s).[23,24] Only C fiber input monosynaptic neurons were measured for further experiments. Measurements were made from only one neuron per slice. The pair pulse protocol was delivered by S88 with 20 Hz frequency and 50 ms pulse interval. The signals were filtered at 2 k Hz. Data were stored on computer by a DigiData 1500 interface and were analyzed by the pCLAMP 10.4 software package (Molecular Devices). All experiments were performed at room temperature.

Statistical analysis

For *in vitro* experiments, the cells were evenly suspended and then randomly distributed in each well tested. For *in vivo* experiments, the animals were distributed into various treatment groups randomly. All of the results are given as means ± SEM. The data were statistically analyzed with two-tailed, paired Student's *t* test and a one-way or two-way ANOVA. When ANOVA showed a significant difference, pairwise comparisons between means were tested by the post hoc Tukey method (SigmaPlot 12.5, San Jose, CA). Significance was set at $p < .05$.

Results

G9a is responsible for nerve injury-induced reductions of MOR, KOR, and DOR in DRG

Peripheral nerve injury increases G9a expression and decreases the expression of MOR, KOR, and DOR in the injured DRG.[4–7,25] To determine whether the increased G9a participated in the downregulation of these three opioid receptors in the DRG following peripheral nerve injury, we carried out a preclinical mouse model of unilateral fourth lumbar (L4) SNL.[14] AAV5-Cre was microinjected into the ipsilateral L4 DRG of $G9a^{fl/fl}$ mice to specifically and selectively knock down the expression of G9a. AAV5-GFP was used as a control. SNL or sham surgery was carried out 35 days after viral injection. The DRGs were harvested for RT-PCR or Western blot analysis seven days after SNL or Sham surgery. AAV5-Cre microinjection produced the deceases in basal levels of *Ehmt2* mRNA (encoding G9a), G9a's two protein isoforms, and H3K9me2 in sham mice and blocked SNL-induced increases in the amounts of *Ehmt2* mRNA, G9a's two protein isoforms, and H3K9me2 in the SNL mice on the ipsilateral side (Figure 1(a)–(c)). Injection of AAV5-Cre, but not AAV5-GFP, reversed reductions of *Oprm1* (encoding MOR), *Oprk1* (encoding KOR), and *Oprd1* (encoding DOR) mRNAs and MOR and KOR proteins in the injured DRG on day 7 post-SNL (Figure 1(a)–(c)). AAV5-Cre injection also markedly increased basal amounts of *Oprm1* mRNA and MOR and KOR proteins in the injured DRG of sham $G9a^{fl/fl}$ mice on day 7 (Figure 1(a)–(c)). Similar results were observed in the injured DRG of G9a conditional knockout (G9aKO) mice that were obtained from the crossbreeding of $G9a^{fl/fl}$ mice with $Avil^{Cre/+}$ mice (Figure 1(d) and (e)). To manipulate G9a activity in DRG, we intrathecally administered BIX-01294 (BIX, 5 μg/10μl), a specific G9a inhibitor[26] in SD rats. BIX was administered once daily for six days after SNL or sham surgery. The ipsilateral L5 DRG was harvested on day 7 post-SNL or sham surgery. As expected, pretreatment with BIX blocked the SNL-induced increase in the level of H3K9me2 in the injured DRG (Figure 1(f)) without affecting basal levels of H3K9me2 in spinal cord and intact DRG (data not shown). BIX significantly restored SNL-induced reductions in the amounts of *Oprm1*, *Oprk1*, and *Oprd1* mRNAs in the injured DRG on day 7 post-SNL (Figure 1(g)). These results indicate that both pharmacological inhibition of DRG G9a and transgenic knockdown of DRG G9a restore the

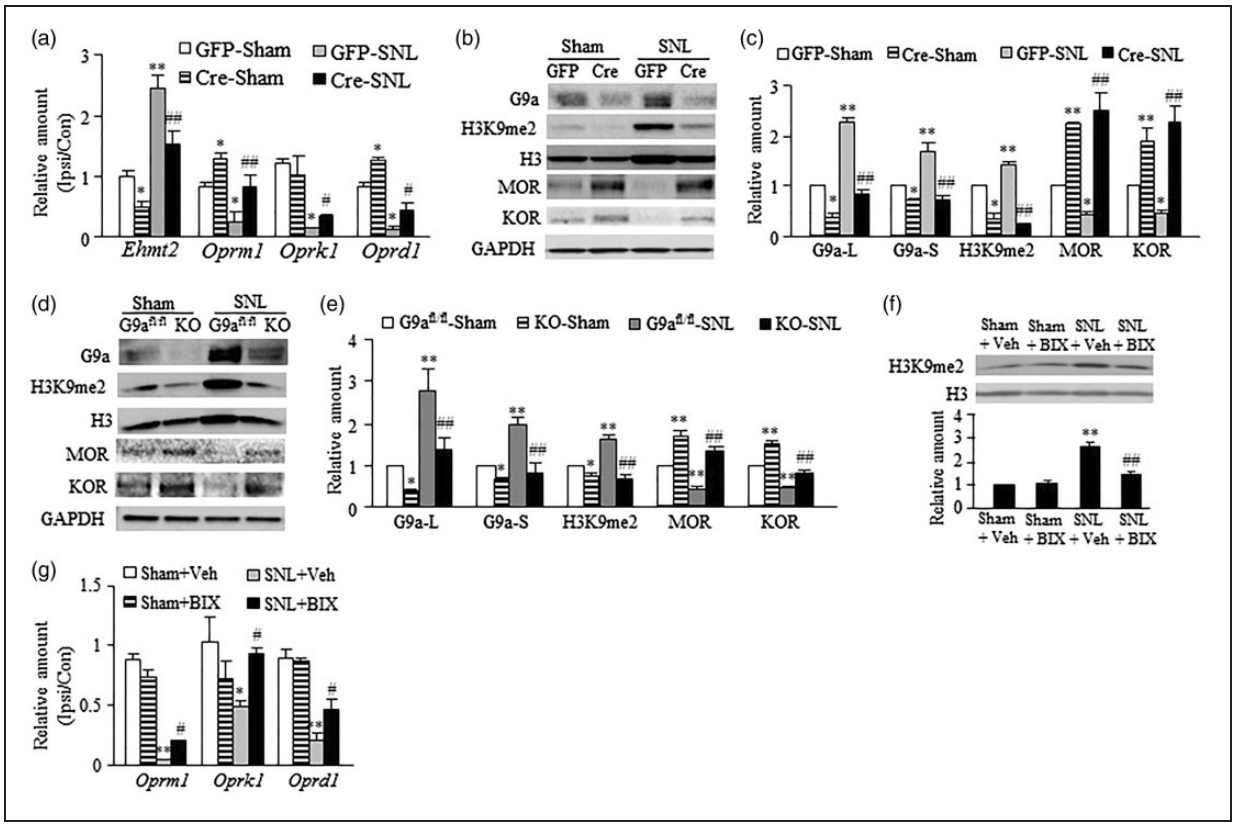

Figure 1. G9a is essential for nerve injury-induced downregulation of opioid receptors in the injured DRG. (**a**–**c**) The amounts of *Ehmt2*, *Oprm1*, *Oprk1*, and *Oprd1* mRNAs in the ipsilateral (Ipsi) and contralateral (Con) L4 DRG (**a**) and the levels of G9a's two protein isoforms, MOR, KOR, and H3K9me2 proteins in the ipsilateral L4 DRG (**b** and **c**) from $G9a^{fl/fl}$ mice with microinjection of AAV5-GFP (GFP) or AAV5-Cre (Cre) into the ipsilateral L4 DRG on day 7 post-SNL or sham surgery. L, long isoform; S, short isoform. n = 12 mice/group for RT-PCR and 6 mice/group for Western blots. $^{*}P < 0.05$ or $^{**}P < 0.01$ *vs* the sham mice injected with AAV5-GFP, $\#P < 0.05$ or $\#\#P < 0.01$ *vs* the SNL mice injected with AAV5-GFP, one-way ANOVA followed by post hoc Tukey test. (**d** and **e**) The levels of G9a's two protein isoforms, H3K9me2, MOR and KOR in the ipsilateral L4 DRG from G9a KO mice and $G9a^{fl/fl}$ mice on day 7 post-SNL or sham surgery. n = 12 mice/group. $^{*}P < 0.05$ or $^{**}P < 0.01$ vs the corresponding sham $G9a^{fl/fl}$ mice, $\#\#P < 0.01$ vs the corresponding SNL $G9a^{fl/fl}$ mice, one-way ANOVA followed by post hoc Tukey test. (**f** and **g**) The level of H3K9me2 in the ipsilateral L4 DRG (**f**) and the amounts of *Oprm1*, *Oprk1*, and *Oprd1* mRNAs in the ipsilateral (Ipsi) and contralateral (Con) L5 DRG (**g**) from mice injected intrathecally with vehicle (Veh) or BIX-01294 (BIX; 2.5 μg/day for 6 days starting at the surgical day) on day 7 after SNL or sham surgery. n = 6 mice/group for Western blots and 12 mice/group for RT-PCR. $^{*}P < 0.05$ or $^{**}P < 0.01$ *vs* the group treated with sham plus vehicle, $\#P < 0.05$ or $\#\#P < 0.01$ *vs* the group treated with SNL plus vehicle, one-way ANOVA followed by post hoc Tukey test.

expression of three opioid receptors in the injured DRG following SNL.

To further confirm our conclusion, we examined the effect of mimicking nerve injury-induced increases in DRG G9a and H3K9me2 through microinjection of a herpes simplex virus (HSV) vector that expresses full-length *Ehmt2* (HSV-G9a) into the L3 and L4 DRG on the expression of MOR, KOR, and DOR in the DRG of naïve mice. HSV-GFP was used as a control. DRG was collected for RT-PCR, Western blot, or immunohistochemical analysis on day 7 post-viral injection. Injection of HSV-G9a, but not HSV-GFP, increased the amounts of *Ehmt2* mRNA, G9a's two protein isoforms, and H3K9me2 and decreased the levels of *Oprm1*, *Oprk1*, and *Oprd1* mRNAs and MOR and KOR proteins in the injected DRG on day 7 post-injection (Figure 2(a) and (b)). The numbers of MOR- and KOR-labeled neurons were also markedly reduced in HSV-G9a-injected DRG compared to those in HSV-GFP-injected DRG (Figure 2(c)). Moreover, single-cell RT-PCR assay revealed the coexpression of *Ehmt2* mRNA with *Oprm1*, *Oprk1*, and *Oprd1* mRNAs in individual small DRG neurons (Figure 2(d)), suggesting that G9a directly regulates *Oprm1*, *Oprk1*, and *Oprd1 gene* expression. Indeed, overexpression of G9a through transduction of HSV-G9a into cultured DRG neurons not only significantly increased the levels of *Ehmt2* mRNA and G9a two protein isoforms as well as H3K9me2 but also reduced the levels of *Oprm1*, *Oprk1*, and *Oprd1* mRNAs and MOR and KOR proteins (Figure 2(e) and (f)). The evidence described above strongly

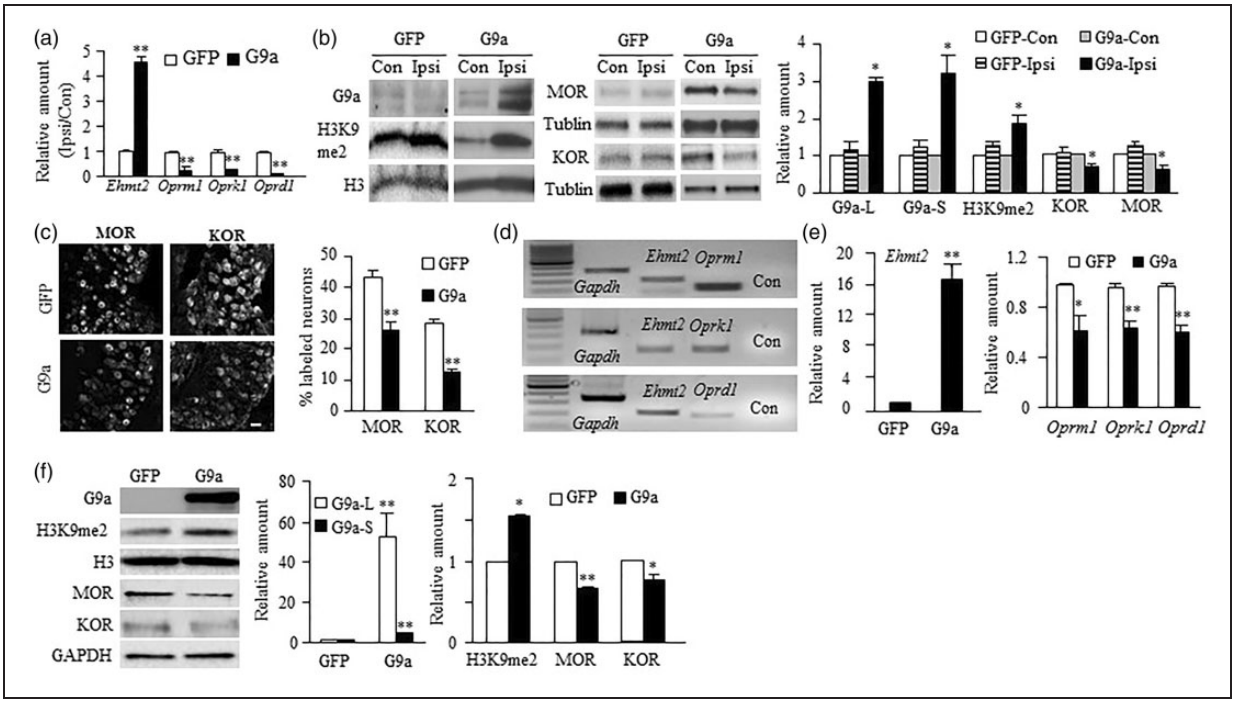

Figure 2. G9a overexpression induced the downregulation of opioid receptors in the DRG. **(a and b)** The amounts of *Ehmt2*, *Oprm1*, *Oprk1*, *Oprd1* mRNAs **(a)** and G9a's two protein isoforms, MOR, KOR, and H3K9me2 proteins (**b**) in the ipsilateral (Ipsi) and contralateral (Con) L3/4 DRG of mice with microinjection of HSV-G9a or HSV-GFP on day 7 post-viral injection. n = 12 mice/group for RT-PCR and 6 mice/group for Western blot. $^{*}P < 0.05$ or $^{**}P < 0.01$ *vs* the corresponding AAV5-GFP-treated group or the corresponding contralateral side by two-tailed paired t-test. (**c**) The expression of MOR- and KOR-labeled neurons in the ipsilateral L4 DRG from mice with microinjection of HSV-G9a or HSV-GFP into this DRG on day 7 after viral injection. Representative immunohistochemical images (left) and a summary of analysis on the number of MOR- and KOR-labeled neurons (right) are shown. n = 3 mice (6 sections/mouse)/group. $^{**}P < 0.01$ *vs* the corresponding HSV-GFP-injected group by two-tailed paired t-test. Scale bar: 25 μm. (**d**) Co-expression of *Ehmt2* mRNA with *Oprm1*, *Oprk1*, and *Oprd1* mRNAs in individual small DRG neurons. *Gapdh* mRNA was used as a positive control. Con, no-DNA. (**e and f**) The amounts of *Ehmt2*, *Oprm1*, *Oprk1*, and *Oprd1* mRNAs (**e**) and G9a's two protein isoforms, MOR, KOR, and H3K9me2 proteins (**f**) in the cultured DRG neurons transduced with HSV-G9a or HSV-GFP. n = 3 repeats. $^{*}P < 0.05$ or $^{**}P < 0.01$ *vs* the corresponding AAV5-GFP-treated group by two-tailed paired t-test.

suggests the contribution of G9a to nerve injury-induced opioid receptor downregulation in the injured DRG.

Increased G9a in the DRG promotes MOR-gated primary afferent neurotransmitter release

MOR is expressed in small-diameter DRG neurons and their primary afferents, especially in peptidergic pain fibers.[27,28] Endogenous opioids acting on MOR exert tonic inhibitory control of neurotransmitter release from these fibers.[21,29] DRG MOR downregulation augments the release of primary afferent neurotransmitters in neuropathic pain.[30,31] Thus, we tested whether mimicking the nerve injury-induced DRG G9a increase altered MOR-gated primary afferent neurotransmitter release. We measured the changes in miniature excitatory postsynaptic current (mEPSC) frequencies, which reflected the alteration in presynaptic neurotransmitter release,[32,33] in lamina II neurons from L3/4 spinal cord slices of mice subjected to injection of HSV-G9a or control HSV-GFP into the ipsilateral L3/4 DRG. The slices were collected five to seven days after DRG microinjection. mEPSC frequency in the HSV-G9a-treated group was significantly higher than that in the control group (Figure 3(a) and (b)), although the mEPSC amplitude was similar between the two groups (Figure 3(a) and (c)). To verify whether this alteration is due to the reduction of MOR function in primary afferents, we applied the selective MOR agonist DAMGO. 1μM of DAMGO led to a greater decrease in mEPSC frequency from the control group ($43.37 \pm 4.05\%$) than that from the HSV-G9a treated group ($19.62 \pm 3.79\%$), although it did not alter the mEPSC amplitude (Figure 3(a)–(c)). This effect was abolished after DAMGO wash out (Figure 3(a)) or by the addition—prior to DAMGO treatment—of the selective MOR antagonist CTOP (data not shown). This evidence suggests that increased G9a expression in DRG results in an increase in MOR-gated presynaptic neurotransmitter release.

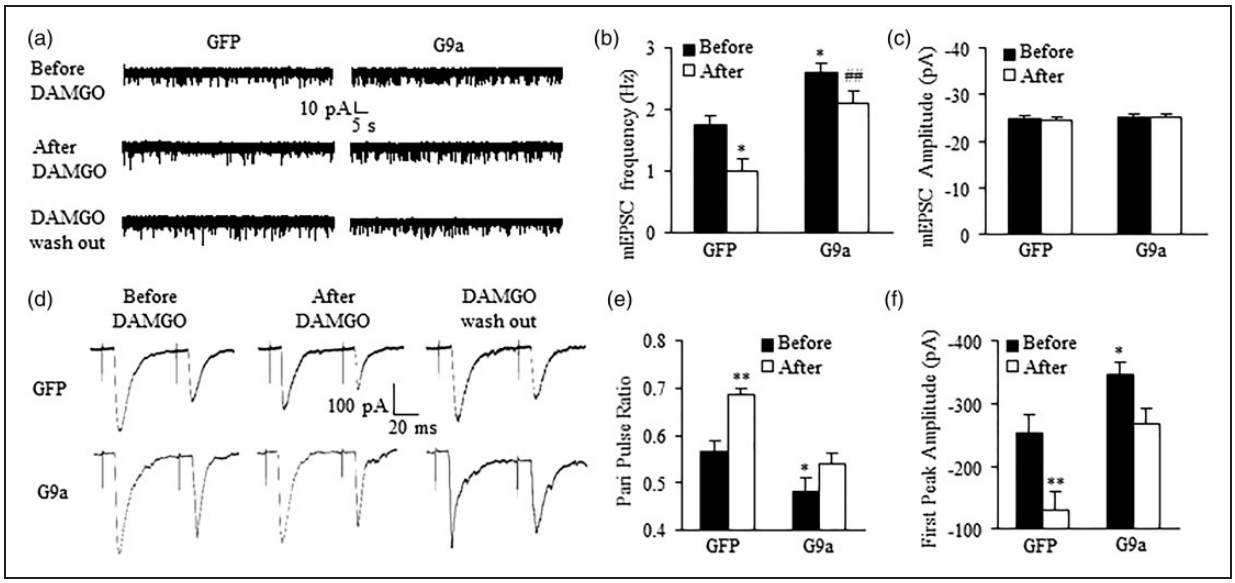

Figure 3. Increase of MOR-gated primary afferent neurotransmitter release in spinal dorsal horn promoted by G9a overexpression in the DRG. Patch clamp recording of lamina II spinal dorsal horn neurons on the ipsilateral side from mice on day 7 after microinjection of HSV-GFP or HSV-G9a into unilateral L3/4 DRG. (**a**) Examples of traces of miniature (m) EPSCs before and after DAMGO (1 μM) application and after DAMGO washout. (**b**) Effect of DAMGO (1 μM) on mEPSC frequencies in the HSV-GFP-injected group (n = 21 neurons, 13 mice) and the HSV-G9a-injected group (n = 21 neurons, 14 mice). $^{*}P < 0.05$ *vs* the HSV-GFP-injected group before DAMGO; $^{\#\#}P < 0.01$ *vs* the HSV-GFP-injected group after DAMGO, one-way ANOVA followed by post hoc Tukey test. (**c**) mEPSC amplitude was not altered in both groups before and after DAMGO application. (**d**) Examples of traces of the C-fiber input recorded before and after DAMGO (1 μM) application and after DAMGO washout. (**e**) Pair pulse ratio (PPR) was significantly decreased in the HSV-G9a-injected group (n = 23 neurons, 19 mice) compared to that in the HSV-GFP-injected group (n = 23 neurons, 20 mice) before DAMGO. DAMGO significantly increased the PPR in the HSV-GFP-injected group, but not in the HSV-G9a-injected group. $^{*}P < 0.05$ or $^{**}P < 0.01$ *vs* the HSV-GFP-injected group before DAMGO, one-way ANOVA followed by post hoc Tukey test. (**f**) The first peak amplitude was significantly increased in the HSV-G9a-injected group compared to the HSV-GFP-injected group before DAMGO. DAMGO dramatically decreased the first peak amplitude in the HSV-GFP-injected group compared to the HSV-G9a-injected group. $^{*}P < 0.05$ or $^{**}P < 0.01$ *vs* the HSV-GFP-injected group before DAMGO, one-way ANOVA followed by post hoc Tukey test.

The mEPSCs recorded above may reflect overall excitatory inputs from both primary afferents and interneurons to the recorded neurons.[33] To further examine the role of G9a in the release of primary afferent neurotransmitters, we recorded the EPSCs evoked by stimulation of the dorsal root (C-fiber: 500 μA intensity and 1 Hz) with a paired pulse protocol. The pair-pulse ratio (PPR), which reflects the probability of primary afferent neurotransmitter release,[32,33] was determined by dividing the second peak amplitude by the first one. PPR significantly declined in the HSV-G9a treated group compared to the control group (Figure 3(d) and (e)). Additionally, the first peak amplitude of the EPSC in the HSV-G9a treated group was higher than that in the control group (Figure 3(d) and (f)). 1μM DAMGO application markedly increased the PPR by 21.24% and decreased the first peak amplitude by 48.99% in the control group, but only 12.43% and 23.31%, respectively, in the HSV-G9a treated group (Figure 3(d)-(f)). DAMGO effects could be abolished after its wash out (Figure 3(d)) or by prior treatment with CTOP (data not shown). These results further demonstrate that increased G9a in DRG promotes neurotransmitter release from primary afferent terminals through presynaptic MOR downregulation in DRG.

Blocking DRG G9a expression improves MOR mediated analgesia, tolerance, and hyperalgesia

We also defined whether MOR-mediated morphine analgesia and tolerance and pain hypersensitivity could be affected by DRG G9a. Given that G9a knockout increased basal expression of MOR in DRG (Figure 1(b)–(e)), we first observed the effect of this knockout on morphine analgesia and morphine-induced tolerance and pain hypersensitivity in naïve mice. For the analgesic effects, thermal test were carried out prior to morphine injection and 30 min after morphine injection five weeks after viral microinjection into the unilateral DRG of $G9a^{fl/fl}$ mice. Injection of AAV5-Cre (but not control AAV5-GFP) into unilateral L3/4 DRG of $G9a^{fl/fl}$ mice robustly increased morphine's MPAE on the ipsilateral (not contralateral) side after subcutaneous (s.c.) administration of a single low dose of morphine

(1 mg/kg) (Figure 4(a)). The morphine-induced pain hypersensitivity was examined five weeks after viral injection. Consistent with previous studies,[16,34] mechanical allodynia, as indicated by the increase in paw withdrawal frequency to von Frey hair stimulation, and thermal hyperalgesia, as indicated by the decrease in paw withdrawal latency to heat stimulation, developed one day after morphine withdrawal in AAV5-GFP-treated G9a$^{fl/fl}$ mice that received repeated injections of s.c. morphine (20 mg/kg, twice daily for eight days) (Figure 4(b) and (c)). In contrast, the AAV5-Cre-treated G9a$^{fl/fl}$ mice failed to display these pain hypersensitivities (Figure 4(b) and (c)). The morphine analgesic tolerance was examined in G9aKO mice. G9a$^{fl/fl}$ mice served as a control group. Repeated s.c. injection of morphine (20 mg/kg, twice daily for eight days) produced morphine analgesic tolerance to a relative low dose of morphine (10 mg/kg) as indicated by time-dependent decreases in morphine MPAEs in control G9a$^{fl/fl}$ mice, but not in the G9aKO mice (Figure 4(d)). The ED_{50} value of morphine in the G9aKO mice (5.4 mg/kg) was substantially smaller than that in control G9a$^{fl/fl}$ mice (9.7 mg/kg) on the last day after repeated s.c. administration of morphine (Figure 4(e)).

Furthermore, we examined whether rescuing MOR downregulation by blocking the nerve injury-induced DRG G9a increase improved morphine analgesia and alleviated morphine-induced tolerance under neuropathic pain conditions. When the first test dose of morphine (3 mg/kg) was administered s.c. on day 6 after SNL, morphine MPAE was much greater in the G9aKO mice than that in control G9a$^{fl/fl}$ mice (Figure 4(f)). Repeated s.c. morphine administration twice daily (20 mg/kg) for four days starting from day 6 after SNL also led to a time-dependent reduction in morphine MPAE in control SNL G9a$^{fl/fl}$ mice (Figure 4(f)), but this reduction was significantly less in the SNL G9aKO mice (Figure 4(f)). The ED_{50} value of morphine was 4.1 mg/kg in the G9aKO mice and 7.2 mg/kg in control G9a$^{fl/fl}$ mice on day 10 post-SNL (Figure 4(g)). Taken together, blocking DRG G9a expression improved morphine analgesia and prevented morphine analgesic tolerance development under neuropathic pain conditions.

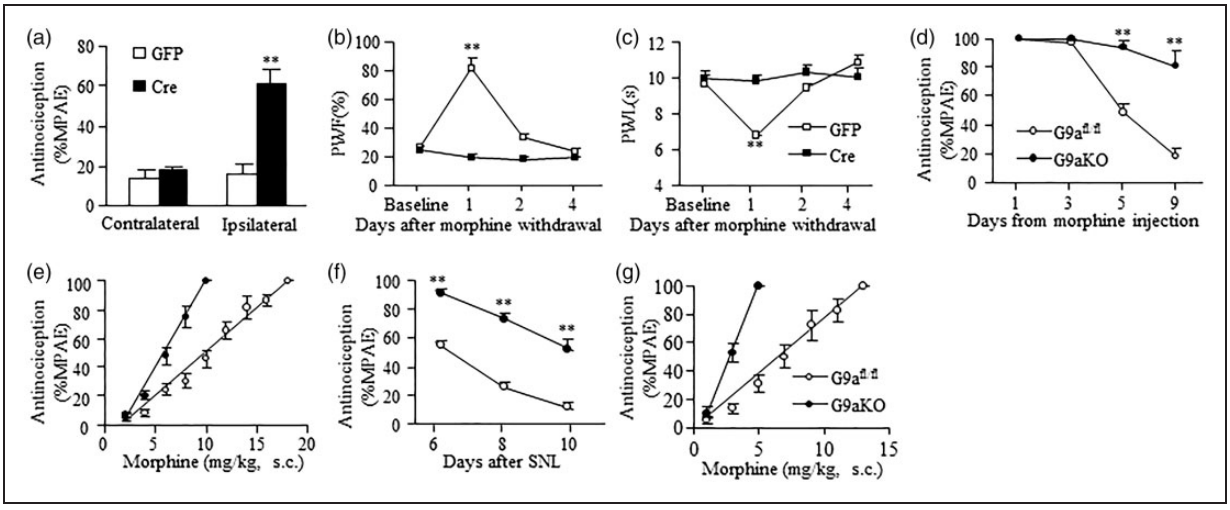

Figure 4. DRG G9a knockout out improves morphine analgesia and prevents morphine tolerance and/or hyperalgesia in naïve or SNL mice. (**a**) The analgesic effect of morphine (1 mg/kg, s.c.) in naïve G9a$^{fl/fl}$ mice with microinjection of AAV5-GFP or AAV5-Cre into unilateral L3/4 DRGs. n = 8–9 mice/group. $^{**}P < 0.01$ *vs* the corresponding AAV5-GFP-injected group by two-tailed paired t-test. (**b** and **c**) Paw withdrawal responses to mechanical (**b**) and thermal (**c**) stimuli on the ipsilateral side after morphine withdrawal in the AAV5-GFP- or AAV5-Cre-injected naïve mice that received repeated morphine injections (20 mg/kg, s.c. twice daily for 8 days). PWF, paw withdrawal frequency. PWL, paw withdrawal latency. n = 5–6 mice/group. $^{**}P < 0.01$ *vs* baseline (before morphine injection), two-way ANOVA followed by post hoc Tukey test. (**d**) Time course of morphine-induced analgesia in naïve G9a$^{fl/fl}$ mice and G9aKO mice that received repeated morphine injections (20 mg/kg, s.c. twice daily for 8 days). MPAE, maximal possible analgesic effect. n = 5–6 mice/group. $^{**}P < 0.01$ *vs* the corresponding G9a$^{fl/fl}$ mice, two-way ANOVA followed by post hoc Tukey test. (**e**) The cumulative dose-response curves of morphine in naïve G9a$^{fl/fl}$ mice and G9aKO mice on day 9 after repeated morphine injections as described above. n = 5–6 mice/group. (**f**) Time course of morphine-induced analgesia in the SNL G9a$^{fl/fl}$ mice and G9aKO mice that received repeated morphine injections (20 mg/kg, s.c. twice daily for 4 days starting on day 6 after SNL). n = 5–6 mice/group. $^{**}P < 0.01$ *vs* the corresponding G9a$^{fl/fl}$ mice, two-way ANOVA followed by post hoc Tukey test. (**g**) The cumulative dose-response curves of morphine in the SNL G9a$^{fl/fl}$ mice and G9aKO mice that received repeated morphine injections as described above.

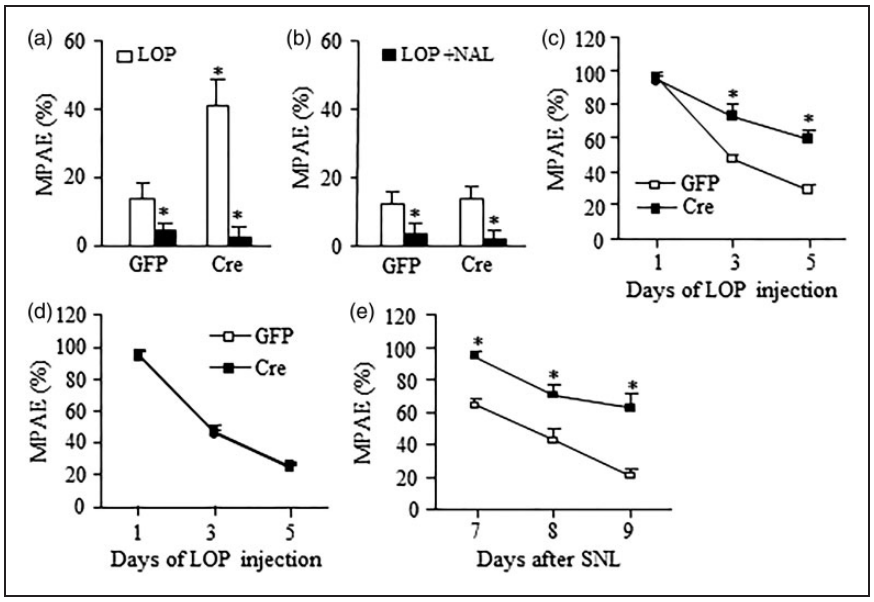

Figure 5. DRG G9a knockout out improves loperamide analgesia and prevents loperamide tolerance in naïve or SNL mice. (**a and b**) The analgesic effect of loperamide (LOP, 2.5 mg/kg, s.c.) in the ipsilateral side **(a)** and contralateral side **(b)** of naïve G9a$^{fl/fl}$ mice with microinjection of AAV5-GFP or AAV5-Cre into unilateral L3/4 DRGs. n = 5 mice/group. This effect can be reversed by Naltrexone (NAL, 5 mg/kg, i.p.). *$P < 0.05$ *vs* the corresponding AAV5-GFP-injected group or LOP alone group by two-tailed paired t-test. (**c** and **d**) Time course of loperamide-induced analgesia in the ipsilateral side **(c)** and contralateral side **(d)** of naïve G9a$^{fl/fl}$ mice with microinjection of AAV5-GFP or AAV5-Cre into unilateral L3/4 DRGs that received repeated loperamide injections (10 mg/kg, s.c. twice daily for 5 days). n = 5 mice/group. **$P < 0.01$ *vs* the corresponding AAV5-GFP-injected group, two-way ANOVA followed by post hoc Tukey test. **(e)** Time course of loperamide-induced analgesia on the ipsilateral side of SNL G9a$^{fl/fl}$ mice with microinjection of AAV5-GFP or AAV5-Cre into unilateral L4 DRGs that received repeated loperamide injections (10 mg/kg, s.c. twice daily for 3 days starting on day 7 after SNL). n = 5 mice/group. **$P < 0.01$ *vs* the corresponding AAV5-GFP-injected group, two-way ANOVA followed by post hoc Tukey test.

To specify DRG G9a regulation on peripheral MOR function, we used a peripheral MOR agonist, loperamide, which cannot pass through the blood–brain barrier.[35] The loperamide analgesic effects and its analgesic tolerance were examined five weeks after DRG viral injection in G9a$^{fl/fl}$ mice. For the analgesic effects, thermal test was carried out before and 30 min after loperamide injection. A low dose of lopermide (2.5 mg/kg, s.c.) produced a dramatic increase in MPAE in the AAV5-Cre injected naïve G9a$^{fl/fl}$ mice compared to control AAV5-GFP injected naïve G9a$^{fl/fl}$ mice on the ipsilateral side (Figure 5(a)). Similar small analgesic effects were seen on the contralateral side in both injected mice (Figure 5(b)). A specific MOR antagonist naltrexone (5 mg/kg, i.p.), which was given 30 min before loperamide administration, could significantly block these effects on the ipsilateral and contralateral sides of both injected mice (Figure 5(a) and (b)). Consistent with a previous report,[17] loperamide analgesic tolerance developed after its systemic and repeated administration (10 mg/kg, twice daily for five days, s.c.) on both microinjected naïve G9a$^{fl/fl}$ mice (Figure 5(c) and (d)). Although the first dose of loperamide produced similar analgesic effects in both microinjected mice, MPAEs decreased at a slower rate in the AAV5-Cre injected mice than that in the AAV5-GFP-injected mice on days 3 and 5 postinjection of loperamide on the ipsilateral side (Figure 5(c)). Similarly, loperamide analgesic tolerance also developed after its systemic and repeated administration (10 mg/kg, twice daily for three days, s.c.) starting on day 7 post-SNL in both microinjected mice. However, the values of MPAEs in the AAV5-Cre injected mice were markedly higher than those in the AAV5-GFP-injected mice on days 7, 8, and 9 post-SNL (Figure 5(e)). These data suggest that rescuing DRG MOR reduction by blocking increased G9a in the injured DRG increases peripheral MOR-triggered analgesic effects and delays the development of peripheral MOR-mediated analgesic tolerance.

Increased G9a blocks the access of CREB to its binding motifs within the Oprm1 gene in the injured DRG after SNL

What is the mechanism by which G9a is involved in DRG MOR reduction under neuropathic pain conditions? We first used ChIP assays and found that G9a binds to two fragments (−450/−288 bp and +142/+312 bp) of the *Oprm1* gene as demonstrated by the amplification of only these two regions (out from

5 regions from −450 to +312 bp) from the complexes immunoprecipitated with G9a antibody in nuclear fractions from sham DRG (Figure 6(a)). These binding activities strikingly increased in the injured DRG on day 7 after SNL, but not after sham surgery (Figure 6(b)). Similar increased bindings of H3K9me2 were also observed in the injured DRG on day 7 after SNL (Figure 6(c)). H3K9me2 binding to these fragments was dependent on G9a expression because DRG G9aKO abolished SNL-induced increases in this binding in SNL mice (Figure 6(c)).

We then determined whether the increased G9a/H3K9me2 binding affected the interactions of the *Oprm1* gene with its transcription factors. The online software (TFSEARCH) prediction revealed a binding motif (+195/+202) of CREB within the 5′-end untranslated region of the gene. ChIP assay confirmed the binding of CREB within this region in the nuclear fractions from DRG after sham surgery or cultured DRG neurons transduced with control AAV5-GFP (Figure 6(d) and 6(e)). This binding was reduced on day 7 following SNL as shown by a 37% reduction in band density in the ipsilateral L4 DRG from the SNL mice compared to that from the sham mice (Figure 6(d)). Consistently, mimicking the SNL-induced increase in DRG G9a in cultured DRG neurons by overexpressing G9a using HSV-G9a abolished the binding of CREB to its binding motif within the *Oprm1* gene (Figure 6(e)). Furthermore, overexpressing CREB via AAV5-CREB in cultured DRG neurons significantly increased levels of MOR protein (Figure 6(f)). This increase was substantially attenuated by coinfection with HSV-G9a (Figure 6(f)). Given that CREB is coexpressed with G9a and MOR in individual DRG neurons (Figure 6(g)), we conclude that the SNL-induced DRG G9a increase leads to the enrichment of H3K9me2 at the specific sites of the *Oprm1* gene, resulting in the blockade of CREB binding to its binding motif within the gene and the silencing of *Oprm1* gene in the injured DRG under neuropathic pain conditions. Interestingly, this blockade of CREB binding to the *Oprm1* gene is persistent despite the fact that SNL time-dependently increases the amounts of CREB and its phosphorylated counterpart in the injured DRG (Figure 6(h)).

Discussion

This study provides the evidence that nerve injury-induced increases in G9a and H3K9me2 are responsible for epigenetic silencing of not only *Oprm1* gene but also *Oprk1* and *Oprd1* genes in the injured DRG. Mimicking these increases downregulated the expression of three opioid receptors in the DRG and promoted the MOR-gated release of primary afferent neurotransmitters. Conversely, blocking these increases rescued DRG *Oprm1*, *Oprd1*, and *Oprk1* gene expression, restored the nerve injury-induced decrease in morphine or loperamide analgesia, and prevented the development of morphine or loperamide-induced analgesic tolerance under neuropathic pain conditions. Mechanistically, nerve injury produced an increase in the binding activity of G9a and H3K9me2 to the *Oprm1* gene, which was associated with reduced binding of CREB to the *Oprm1* gene in the injured DRG. Thus, G9a participates in the nerve injury-induced reduction of MOR likely through G9a-triggered blockage in the access of CREB to the *Oprm1* gene.

G9a as a repressor of gene expression participates in the nerve injury-induced reduction of opioid receptors in the injured DRG. A recent study reported that G9a was required for nerve injury-induced downregulation of the *Oprm1* gene in the injured DRG.[11] Nerve injury increased the enrichment of H3K9me2 in regions (−43/+63 bp, −411/−302 bp, and +376/+495 bp) of the *Oprm1* gene in the DRG.[11] G9a inhibition or knockdown rescued MOR expression in the injured DRG and morphine analgesic effects reduced by SNL.[11] However, whether G9a also regulates other opioid receptors is unknown. Furthermore, the mechanism of how G9a is involved in nerve injury-induced DRG *Oprm1* gene silencing is unclear. We demonstrated here that G9a was essential for epigenetic silencing of not only the *Oprm1* gene but also *Oprk1* and *Oprd1* genes in the injured DRG under neuropathic pain conditions. SNL-induced reductions of these opioid receptors could be rescued by G9a knockdown/knockout in the injured DRG and mimicked by DRG G9a overexpression. Moreover, DRG G9a knockdown/knockout restored the nerve injury-induced decrease in morphine or loperamide analgesia and prevented the development of morphine or loperamide-induced analgesic tolerance following SNL, whereas DRG G9a overexpression enhanced the MOR-gated release of primary afferent neurotransmitters. Mechanistically, G9a binds to only two regions (−450/−288 bp and +142/+312 bp) out of five regions (from −450 bp to +312 bp) of the *Oprm1* gene. SNL increased the binding activity of G9a and H3K9me2 to these two regions. These findings suggest that the increased enrichment of histone methylation by G9a is distributed in specific sites within the promoter and 5′-end untranslated regions of the *Oprm1* gene following SNL. The distinct binding sites of H3K9me2 observed between the present study and a previous study[11] may be due to species difference (mouse vs rat). It should be noted that other histone methyltransferases such as SUV39H1 may be responsible for the production of H3K9me2 after SNL.[36]

We further found that the increased binding of G9a/H3K9me2 to the *Oprm1* gene was associated with the decreased binding of CREB to its motif within the

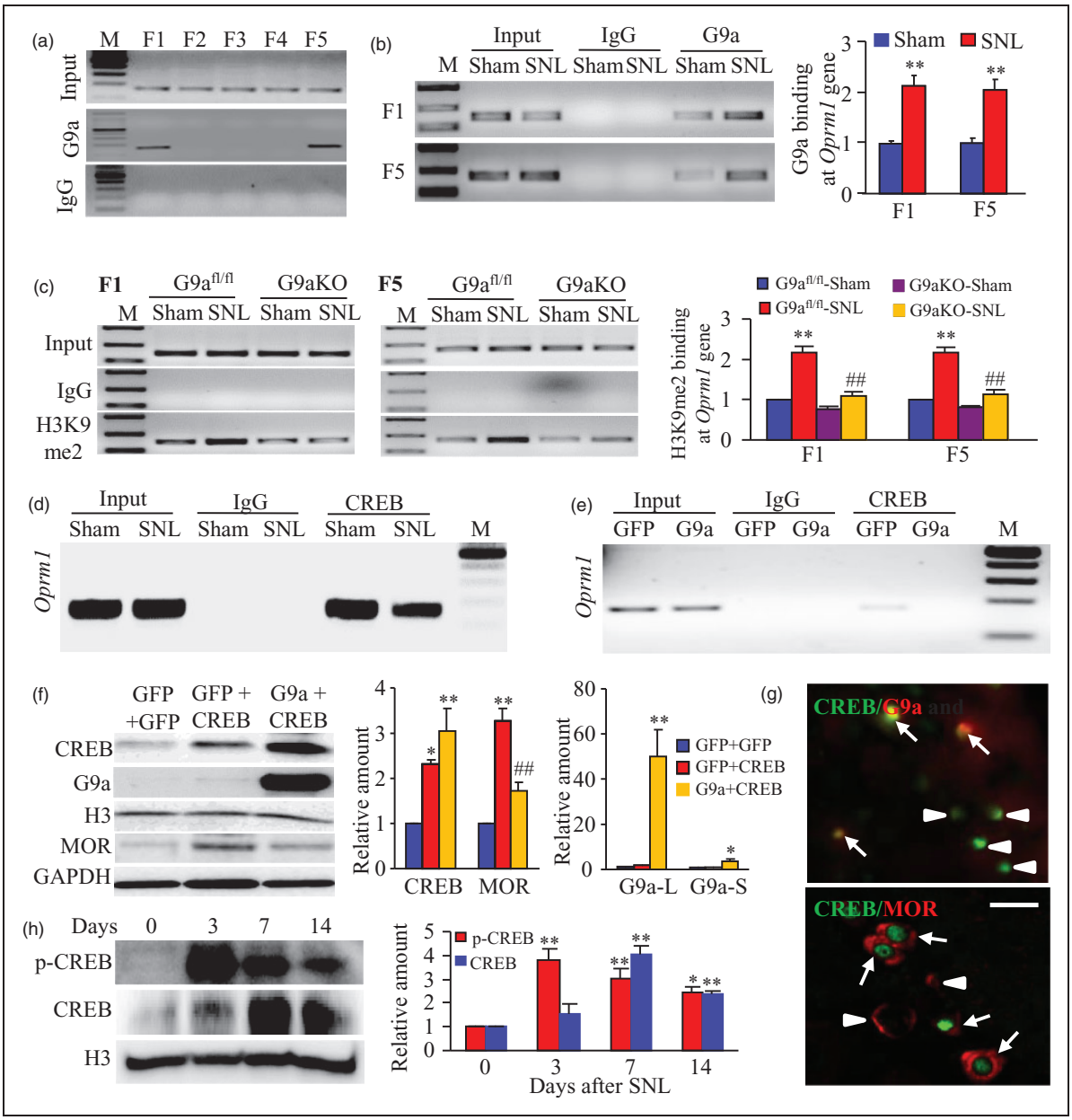

Figure 6. Increased G9a is associated with reduced binding of CREB to its binding motif within the *Oprm1* gene in the injured DRG after SNL. (**a**) Two fragments (F1, −450/−280 bp; F5, +142/+312 bp), but not other fragments (F2, −310/−143 bp; F3, −164/−6 bp; F4, −7/+166 bp), from the promoter and 5'-end untranslated regions of the *Oprm1* gene were immunoprecipitated by the rabbit anti-G9a (not by rabbit normal IgG) in rat DRGs. Input, total purified fragments. M, ladder marker. n = 3 repeats. (**b**) G9a bindings to F1 and F5 fragments within the *Oprm1* gene in the injured DRGs on day 7 post-SNL or sham surgery. n = 9 rats/group. $^{**}P < 0.01$ *vs* the corresponding sham group by two-tailed paired t-test. (**c**) H3K9me2 bindings to F1 (−483/−320) and F5 (+163/+358) fragments within the *Oprm1* gene in the injured DRGs of G9a$^{fl/fl}$ mice and G9aKO mice on day 7 post-SNL or sham surgery. n = 15 mice/group. $^{**}P < 0.01$ *vs* the corresponding sham G9a$^{fl/fl}$ mice. $^{\#\#}P < 0.05$ *vs* the corresponding SNL G9a$^{fl/fl}$ mice, one-way ANOVA followed by post hoc Tukey test. (**d** and **e**) The fragment of *Oprm1* gene including putative CREB binding motif immunoprecipitated by the rabbit anti-CREB, but not by rabbit normal IgG, in the ipsilateral L4 DRG on day 7 after SNL or sham surgery (**d**) or in the cultured mouse DRG neurons transduced with HSV-G9a or HSV-GFP (**e**). Input, total purified fragments. M, ladder marker. n = 3 repeats/model or transduction. (**f**) The amounts of CREB, G9a long (L) and short (S) isoforms, and MOR proteins in the cultured mouse DRG neurons transduced with HSV-GFP plus AAV5-GFP, HSV-GFP plus AAV5-CREB, or HSV-G9a plus AAV5-CREB. Representative Western blots (left) and a summary of densitometric analysis (right) are shown. n = 3 repeats. $^{*}P < 0.05$ or $^{**}P < 0.01$ *vs* the corresponding HSV-GFP plus AAV5-GFP group, $^{\#\#}P < 0.01$ *vs* the corresponding HSV-GFP plus AAV5-CREB group, one-way ANOVA followed by post hoc Tukey test. (**g**) Representative examples showing the co-localization of CREB with G9a or MOR in the DRG neurons (arrows). Arrowheads, single CREB- or MOR-labeled DRG neurons. Scale bar: 25 μm. (**h**) The levels of phosphorylated (p-) CREB and CREB proteins in the ipsilateral L4 DRG after SNL. Representative Western blots (left) and a summary of densitometric analysis (right) are shown. n = 6 mice/time point. $^{*}P < 0.05$ or $^{**}P < 0.01$ *vs* the corresponding control group (0 day), one-way ANOVA followed by post hoc Tukey test.

Oprm1 gene. CREB overexpression increased MOR expression that could be attenuated by co-G9a overexpression in cultured DRG neurons. Nerve injury-induced reduction of the *Oprm1* gene was dependent on the increase of G9a, but not CREB, in the injured DRG. Thus, G9a-participated reduction of DRG MOR is mediated likely through G9a-triggered production of *H3K9me2* to block the access of CREB to the *Oprm1* gene in the injured DRG neurons under neuropathic pain conditions. Whether similar mechanisms by which G9a is involved in nerve injury-induced silencing of *Oprk1* and *Oprd1* genes in the injured DRG exist remains to be determined.

Multiple epigenetic mechanisms may be involved in nerve injury-induced reduction of the DRG *Oprm1* gene. In addition to G9a-triggered histone modification described above, DNA methylation and transcriptional repressors may also contribute to the decreased MOR expression in the injured DRG after peripheral nerve injury.[7,37] Peripheral nerve injury increased DNA methylation, promoted a transcriptional repressor neuron-restrictive silencer factor (NRSF) binding to the neuron-restrictive silencer element, and decreased NRSF-mediated H3/4 acetylation within the *Oprm1* gene.[7,37] Pharmacological blockage of DNA methylation rescued a decrease in expression of DRG MOR and improved systemic, spinal, and peripheral morphine analgesia.[7] NRSF knockdown rescued nerve injury-induced downregulation of DRG MOR and attenuated the loss of peripheral morphine analgesia.[37] It has been demonstrated that G9a interacts with DNA methyltransferases to coordinate histone and DNA methylation.[38] Our recent work showed that nerve injury-induced increase in one DNA methyltransferase, DNMT3a, was essential for the silencing of *Oprm1* and *Oprk1* genes in the injured DRG after SNL (data not shown). It is very likely that these epigenetic mechanisms interact with each other to regulate DRG MOR expression under neuropathic pain conditions.

G9a plays a critical role in neuropathic pain genesis. Blocking SNL-induced G9a increase in the injured DRG attenuated the development of SNL-induced pain hypersensitivity.[25] Our recent work showed that knockdown or knockout of DRG G9a produced an antinociceptive effects following SNL and that mimicking SNL-induced DRG G9a increase led to neuropathic pain symptoms (data not shown). The involvement of DRG G9a in nerve injury-induced pain hypersensitivity may be related to its participation in nerve injury-induced downregulation of voltage-gated potassium channels and opioid receptors in the injured DRG. G9a inhibition restored the expression of *Oprm1*, *Kcna4*, *Kcnd2*, *Kcnq2*, and *Kcnma1* genes in the injured DRG.[11,25] The present study demonstrated that knockdown or knockout of DRG G9a rescued the expression of *Oprm1*, *Oprk1*, and *Oprd1* in the injured DRG. DRG G9a overexpression reduced these opioid receptor expression in the DRG and promoted primary neurotransmitter release. Given that voltage-gated potassium channels and opioid receptors control DRG neuronal excitability and primary afferent neurotransmitter release,[4,5,12,13] G9a contributes to neuropathic pain likely by silencing expression of these potassium channels and opioid receptors in the injured DRG. More interestingly, we observed that DRG G9a knockdown attenuated analgesic tolerance caused by repeated injections of morphine or loperamide in naïve or SNL mice. This effect is attributed to an increase of basal level of DRG MOR under normal conditions and a rescue of DRG MOR expression under neuropathic pain conditions following DRG G9a knockdown. A previous study reported that repeated injections of morphine reduced G9a expression in mouse nucleus accumbens.[39] In contrast, our data indicate no significant change in DRG G9a expression during chronic morphine or loperamide exposure in control (GFP-injected) mice (data not shown). Consistently, these control mice displayed full development of morphine or loperamide analgesic tolerance. It is evident that chronic morphine may have distinct effect on G9a expression in the regions of nerve system.

In summary, the present study demonstrated a G9a-triggered epigenetic mechanism of how nerve injury downregulates the expression of opioid receptors in the injured DRG. Given that DRG G9a inhibition or knockout not only rescues morphine or loperamide analgesia, reduces primary afferent transmitter release and prevents morphine or loperamide-induced analgesic tolerance but also attenuates neuropathic pain[25] under neuropathic pain conditions, the clinical development of G9a inhibitors will likely have the benefits of antinociception and anti-opioid tolerance in neuropathic pain management.

Acknowledgments

The authors thank Eric J Neslter (Icahn School of Medicine at Mount Sinai) for G9a flox mice, HSV-G9a, and HSV-GFP virus; Fan Wang (Duke University Medical Center) for Advillin$^{Cre/+}$ mice; and Han-Rong Weng (University of Georgia College of Pharmacy) for electrophysiological data analysis.

Author Contributions

YXT conceived the project and supervised all experiments. LL, JYZ, XG, SW, and YXT assisted with experimental design. LL, JYZ, XG, KM, and SW carried out animal surgery and molecular, biochemical, and behavioral experiments. XG performed patch clamp recording. LL, JYZ, XG, SW, MX, AB, and YXT analyzed the data. YXT wrote the manuscript. All authors read and discussed the manuscript. LL, JYZ, and XG contributed equally to this study.

Declaration of Conflicting Interests

The author(s) declared no potential conflicts of interest with respect to the research, authorship, and/or publication of this article.

Funding

The author(s) disclosed receipt of the following financial support for the research, authorship, and/or publication of this article: This work was supported by NIH Grants (DA033390, NS094664, NS094224 and HL117684).

References

1. van HO, Austin SK, Khan RA, et al. Neuropathic pain in the general population: a systematic review of epidemiological studies. *Pain* 2014; 155: 654–662.
2. O'Connor AB. Neuropathic pain: quality-of-life impact, costs and cost effectiveness of therapy. *Pharmacoeconomics* 2009; 27: 95–112.
3. Bekhit MH. Opioid-induced hyperalgesia and tolerance. *Am J Ther* 2010; 17: 498–510.
4. Kohno T, Ji RR, Ito N, et al. Peripheral axonal injury results in reduced mu opioid receptor pre- and post-synaptic action in the spinal cord. *Pain* 2005; 117: 77–87.
5. Lee CY, Perez FM, Wang W, et al. Dynamic temporal and spatial regulation of mu opioid receptor expression in primary afferent neurons following spinal nerve injury. *Eur J Pain* 2011; 15: 669–675.
6. Obara I, Parkitna JR, Korostynski M, et al. Local peripheral opioid effects and expression of opioid genes in the spinal cord and dorsal root ganglia in neuropathic and inflammatory pain. *Pain* 2009; 141: 283–291.
7. Zhou XL, Yu LN, Wang Y, et al. Increased methylation of the MOR gene proximal promoter in primary sensory neurons plays a crucial role in the decreased analgesic effect of opioids in neuropathic pain. *Mol Pain* 2014; 10: 51.
8. Liang L, Lutz BM, Bekker A, et al. Epigenetic regulation of chronic pain. *Epigenomics* 2015; 7: 235–245.
9. Shinkai Y and Tachibana M. H3K9 methyltransferase G9a and the related molecule GLP. *Genes Dev* 2011; 25: 781–788.
10. Kouzarides T. Chromatin modifications and their function. *Cell* 2007; 128: 693–705.
11. Zhang Y, Chen SR, Laumet G, et al. Nerve injury diminishes opioid analgesia through lysine methyltransferase-mediated transcriptional repression of mu-opioid receptors in primary sensory neurons. *J Biol Chem* 2016; 291: 8475–8485.
12. Li Z, Gu X, Sun L, et al. Dorsal root ganglion myeloid zinc finger protein 1 contributes to neuropathic pain after peripheral nerve trauma. *Pain* 2015; 156: 711–721.
13. Zhao X, Tang Z, Zhang H, et al. A long noncoding RNA contributes to neuropathic pain by silencing Kcna2 in primary afferent neurons. *Nat Neurosci* 2013; 16: 1024–1031.
14. Rigaud M, Gemes G, Barabas ME, et al. Species and strain differences in rodent sciatic nerve anatomy: implications for studies of neuropathic pain. *Pain* 2008; 136: 188–201.
15. Liang L, Fan L, Tao B, et al. Protein kinase B/Akt is required for complete Freund's adjuvant-induced upregulation of Nav1.7 and Nav1.8 in primary sensory neurons. *J Pain* 2013; 14: 638–647.
16. Liaw WJ, Zhu XG, Yaster M, et al. Distinct expression of synaptic NR2A and NR2B in the central nervous system and impaired morphine tolerance and physical dependence in mice deficient in postsynaptic density-93 protein. *Mol Pain* 2008; 4: 45.
17. He SQ, Yang F, Perez FM, et al. Tolerance develops to the antiallodynic effects of the peripherally acting opioid loperamide hydrochloride in nerve-injured rats. *Pain* 2013; 154: 2477–2486.
18. Xu JT, Zhao JY, Zhao X, et al. Opioid receptor-triggered spinal mTORC1 activation contributes to morphine tolerance and hyperalgesia. *J Clin Invest* 2014; 124: 592–603.
19. Tao YX, Rumbaugh G, Wang GD, et al. Impaired NMDA receptor-mediated postsynaptic function and blunted NMDA receptor-dependent persistent pain in mice lacking postsynaptic density-93 protein. *J Neurosci* 2003; 23: 6703–6712.
20. Ataka T, Kumamoto E, Shimoji K, et al. Baclofen inhibits more effectively C-afferent than Adelta-afferent glutamatergic transmission in substantia gelatinosa neurons of adult rat spinal cord slices. *Pain* 2000; 86: 273–282.
21. Heinke B, Gingl E and Sandkuhler J. Multiple targets of mu-opioid receptor-mediated presynaptic inhibition at primary afferent Adelta- and C-fibers. *J Neurosci* 2011; 31: 1313–1322.
22. Ikoma M, Kohno T and Baba H. Differential presynaptic effects of opioid agonists on Adelta- and C-afferent glutamatergic transmission to the spinal dorsal horn. *Anesthesiology* 2007; 107: 807–812.
23. Nakatsuka T, Park JS, Kumamoto E, et al. Plastic changes in sensory inputs to rat substantia gelatinosa neurons following peripheral inflammation. *Pain* 1999; 82: 39–47.
24. Torsney C and MacDermott AB. Disinhibition opens the gate to pathological pain signaling in superficial neurokinin 1 receptor-expressing neurons in rat spinal cord. *J Neurosci* 2006; 26: 1833–1843.
25. Laumet G, Garriga J, Chen SR, et al. G9a is essential for epigenetic silencing of K(+) channel genes in acute-to-chronic pain transition. *Nat Neurosci* 2015; 18: 1746–1755.
26. Malmquist NA, Moss TA, Mecheri S, et al. Small-molecule histone methyltransferase inhibitors display rapid antimalarial activity against all blood stage forms in *Plasmodium falciparum*. *Proc Natl Acad Sci USA* 2012; 109: 16708–16713.
27. Ji RR, Zhang Q, Law PY, et al. Expression of mu-, delta-, and kappa-opioid receptor-like immunoreactivities in rat dorsal root ganglia after carrageenan-induced inflammation. *J Neurosci* 1995; 15: 8156–8166.
28. Scherrer G, Imamachi N, Cao YQ, et al. Dissociation of the opioid receptor mechanisms that control mechanical and heat pain. *Cell* 2009; 137: 1148–1159.
29. Taddese A, Nah SY and McCleskey EW. Selective opioid inhibition of small nociceptive neurons. *Science* 1995; 270: 1366–1369.
30. Sehgal N, Smith HS and Manchikanti L. Peripherally acting opioids and clinical implications for pain control. *Pain Physician* 2011; 14: 249–258.

31. Stein C and Lang LJ. Peripheral mechanisms of opioid analgesia. *Curr Opin Pharmacol* 2009; 9: 3–8.
32. Weng HR, Chen JH, Pan ZZ, et al. Glial glutamate transporter 1 regulates the spatial and temporal coding of glutamatergic synaptic transmission in spinal lamina II neurons. *Neuroscience* 2007; 149: 898–907.
33. Yan X and Weng HR. Endogenous interleukin-1beta in neuropathic rats enhances glutamate release from the primary afferents in the spinal dorsal horn through coupling with presynaptic N-methyl-D-aspartic acid receptors. *J Biol Chem* 2013; 288: 30544–30557.
34. Li X, Angst MS and Clark JD. A murine model of opioid-induced hyperalgesia. *Brain Res Mol Brain Res* 2001; 86: 56–62.
35. Guan Y, Johanek LM, Hartke TV, et al. Peripherally acting mu-opioid receptor agonist attenuates neuropathic pain in rats after L5 spinal nerve injury. *Pain* 2008; 138: 318–329.
36. Zhang J, Liang L, Miao X, et al. Contribution of the suppressor of variegation 3–9 Homolog 1 in dorsal root ganglia and spinal cord dorsal horn to nerve injury-induced nociceptive hypersensitivity. *Anesthesiology* 2016; 125: 765–778.
37. Uchida H, Ma L and Ueda H. Epigenetic gene silencing underlies C-fiber dysfunctions in neuropathic pain. *J Neurosci* 2010; 30: 4806–4814.
38. Esteve PO, Chin HG, Smallwood A, et al. Direct interaction between DNMT1 and G9a coordinates DNA and histone methylation during replication. *Genes Dev* 2006; 20: 3089–3103.
39. Sun H, Maze I, Dietz DM, et al. Morphine epigenomically regulates behavior through alterations in histone H3 lysine 9 dimethylation in the nucleus accumbens. *J Neurosci* 2012; 32: 17454–17464.